Open-source `nanoFluid4Foam` Toolbox for CFD Simulation of Mono and Hybrid nanofluid

Ehsan Golab[a, b], Behzad Vahedi[b]

[a] Department of Mechanical Engineering, Sharif University of Technology (SUT), Tehran, Iran

[b] Functional Neurosurgery Research Center, Shahid Beheshti University of Medical Sciences

Abstract

Inclusion of nanoparticles into a base fluid called nanofluid is a promising way to improve the thermophysical properties of a base fluid as well as heat transfer rate or even is applicable for drug delivery in cardiovascular systems and has attracted so many attentions since three decades ago. Nanofluids are categorized into two main subcategories: mono nanofluid, consisting of one type of nanoparticle and hybrid nanofluid, comprised of different types of particles. Over the past three decades, ample different analytical and experimental models of the thermophysical properties of nanofluids, especially dynamic viscosity and thermal conductivity have been proposed by researchers. In this regard, existing gaps in these areas provide the authors of the present study with an incentive to develop a toolbox, including a variety of different models for dynamic viscosity and thermal conductivity. Also, considering the nanoparticles transport has always been a controversial issue. In this vein, the programmed toolbox possesses the ability to solve the mass transport equation by considering two decisive mechanisms: Brownian and thermophoresis diffusions. For thermophoresis term, different models have been incorporated. In addition to nanoparticles, in the last decade, a novel particle called micro/nano encapsulated phase change materials (M/N-EPCM) was introduced made of two main parts: a phase change material-based core and shell. These particles have also been implemented in the

nanoFluid4Foam toolbox. Moreover, many applicable boundary conditions such as waveform and Womersley velocity for cardiovascular problems, non-uniform heat flux for parabolic trough collector were programmed and implemented in this toolbox. This object-oriented toolbox has been prepared for the OpenFOAM package, encompassing three parts: libraries, solvers, and tutorials. Finally, different eminent experimental studies for forced and natural convections, as well as phase change materials melting, have been simulated to validate the current toolbox.

Keywords: Nanofluid; OpenFOAM; Open-source toolbox; C++; nanoFluid4Foam.

1. Introduction

Gone are the days when the conventional heat transfer fluids had played crucial role in the design of thermal systems. Since three decades ago, thanks to the introduction of a new class of heat transfer fluids, nanofluids, the design of many thermal and heat transfer systems has shifted from low to highly efficient systems. Adding solid particles into a fluid was theoretically performed by Maxwell for the first time [1]. Choi et al. [2] was a pioneer in proposing the term "nanofluids". Nanofluids are suspensions of dispersed nano-sized particles (nanoparticles, nanofibers, nanotubes, nanowires, nanorods, nanosheet, or droplets) injected into a base fluid [3]. These nanoscale-sized particles are classified in terms of different materials as follows: metals (*Al, Cu, Ag, Au, Ti, Fe,* etc.), metal oxides (Al_2O_3, *CuO*, TiO_2, *ZnO* etc.), carbon-based (SWCNT, MWCNT, diamond, and graphene), nitrides, and carbides. The inclusion of these nano-sized particles into a host fluid greatly boosts the thermophysical properties of the conventional heat transfer fluids and have drawn many attentions due to their unique thermophysical properties, especially thermal conductivity. The addition of them also sets the stage for heat transfer rate

enhancement in a thermal system. The more nanoparticles are injected into a base fluid, the higher the heat transfer enhancement would be. However, if used excessively, nanoparticles would have deleterious impacts on thermal systems. Hence, to acquire an appropriate heat transfer rate augmentation, different factors including size, shape, and concentration should be considered before utilizing them. Xuan and Li [4] reported that adding concentration of 5% of nanoparticles increased the effective thermal conductivity of the host fluid by at least 20%. Their applications are mostly in electronic (cooling of microchips), automotive (nanofluid coolant, engine oils, lubricants), renewable energy (solar and geothermal energy), and biomedicine (drug delivery and cancer therapy) [5].

Another promising material to meet the urgent needs of the energy in world are phase change materials (PCMs). Given that inherently used in solid-liquid transition phase, PCMs possess the ability to gain, store, and release a ridiculous amount of energy. They receive the heat as sensible heat until their temperature approach to the temperature of the melting, which the heat would be stored as latent heat [6]. Solid-liquid PCMs are second to none owing to their larger heat storage capacity and lesser volume change during phase change [7]. Yet, their uses are associated with two main problems: high viscosity and low thermal conductivity. In order to mitigate issues mentioned before, one procedure is proposed: encapsulation. Encapsulation refers to a method that PCMs are surrounded by a solid shell known as encapsulated phase change material (EPCM) particles. Based on their sizes, they are mainly classified into two groups: micro-EPCM and nano-EPCM. The core is mostly made of organic (paraffins, alcohols, and esters), inorganic (salts, salts hydrate, metal alloys, and metallic compounds), and eutectic. The shell also is chosen based on different criteria, but they are chiefly comprised of organic (melamine and urea formaldehyde resins) inorganic (Silica, Zinc oxide, Titanium oxide, Aluminum, and so on), and

organic-inorganic hybrid [8]. M/N-EPCMs are widely used in many different areas such as medicine and food transportation, solar heating, building conditioning, solar water heaters, fire protection, industrial refrigeration, textile industries, renewable energy harnessing, and so on [9].

The use of mono nanofluid, a fluid made up of one type of nanoparticle such as metal particles, CNT, or M/N-EPCM has some drawbacks, including limited thermal conductivity augmentation and aggregation. According to recent studies, although the inclusion of nanoparticles has yielded thermal conductivity augmentation, some types of nanoparticles, such as metallic oxides unlike metallic and carbon-based have shown insignificant changes in thermal conductivity of the base fluid [10]. Besides, when utilized, it is highly probable that metallic nanoparticles would be clustered, so adding ceramic nanoparticles is a remedy to prevent clustering phenomena. Moreover, in some applications, there is a need to simultaneously store a vast amount of energy and increase the thermal conductivity without temperature enhancement. In order to solve the issues mentioned, researchers have devised a new strategy called hybrid nanofluid. A hybrid nanofluid is a suspension comprised of at least two distinct types of nanoparticles (metallic with metallic oxide, metallic oxide with carbon-based, metallic with M/N-EPCM, and so on) in a host fluid [11].

The addition of nanoparticles is associated with a variation in the thermophysical properties of the host fluid. Since the density and specific heat capacity of nanofluid have a linear relationship with the volume fraction of nanoparticles, a limited number of studies have been performed [12]. On the contrary, numerous experimental and theoretical studies have proposed different correlations for the thermal conductivity and dynamic viscosity of nanofluids since the thermal conductivity and dynamic viscosity depend on a wide range of parameters, including particle

size, shape, material, and volume fraction, as well as the base fluid material and temperature [13].

Nanofluid flow and heat transfer are chiefly modeled in two ways: the single-phase and two-phase models. In single-phase modeling, particles are considered to be homogenously distributed in the base fluid, and the relative velocity between the two phases is assumed to be zero. In two-phase modeling, mass, momentum, and energy equations are handled differently for each phase. The most common and fully fledged two-phase models are the Lagrangian-Eulerian model (LEM), the Eulerian- Mixture model (EMM), the Eulerian-Eulerian model (EEM), and Buongiorno's model (BGM) [14]. The LEM method produces accurate results, but it has a high computational cost. In the EMM method, the energy and momentum equations coupled with continuity are solved for the mixture phase, and then phase velocities are acquired based on empirical correlation. In the EEM method, not only continuity, momentum, and energy equations are solved for each phase, but also the interaction between phases is included [15]. Of all the methods mentioned before, BGM has revealed not only reasonable precision but also a lower run time. Buongiorno thought differently and attributed the heat transfer enhancement of nanoparticles' injection to other reasons besides the thermal conductivity improvement. He elucidated the fact that seven slip mechanisms, including inertia, Brownian diffusion, thermophoresis, diffusiophoresis, the Magnus effect, fluid drainage, and gravity, play an important role in having relative velocity between particles and the host fluid [16]. Of all mechanisms, thermophoresis and Brownian forces owing to temperature and concentration gradients are of great importance in nanofluids. Vahedi et al. [19] and Sayyar et al. [20], nevertheless, shed light on the fact that the results of BGM and the single-phase model (SPM)

are virtually the same, especially in turbulent regimes. In fact, implementing BGM is only beneficial when the distribution of nanoparticles is important.

Thermal properties of nanofluids are viewed through thermodynamic and computational fluid dynamics lenses. Thermodynamically speaking, the properties are not investigated comprehensively, but in CFD studies, the thermal properties depend on the operation of the studied system. In this respect, the calculation of thermophysical properties of nanofluids is a vital step in CFD problems dealing with heat transfer processes.

The foundation of OpenFOAM was laid at the Imperial College, London. Then, by taking advantage of one of the exceptional features of the C++ programming language, object-orientated, it was developed and released under the GPL license [21]. OpenFOAM stands for open field operation and manipulation concept. The aim was to generating a high-level syntax and general toolbox for solving PDEs associated with parallel computing while it is open source and free [22]. OpenFOAM has been adopted in many different settings given that it facilitates simulating a broad spectrum of problems from combustion, heat transfer, turbulence, and multiphase flows to electromagnetics, acoustics, and even finance [23]. Many researchers and companies all around the world have become interested in using OpenFOAM owing to its affordability and reliability. For instance, OpenCFD has received a governmental grant to perform simulations aimed at understanding the underlying concept of COVID-19 transmission in public areas and proposing possible solutions to keep it in check [24].

2. Toolbox structure and design

Gone are the days when complex mathematical partial differential equations, especially Navier-Stokes equations, had been analytically solved considering too many assumptions. Today, thanks to the emergence of new numerical methods and computers, a wide array of complicated computational fluid mechanics problems are solved more conveniently. Moreover, the early computers used to have a low-level and hard-to-understand programming language called assembly language, and then, since the late 20th century, other straightforward languages have emerged. Various numerical procedures with different programming languages have appeared. In this regard, a great number of CFD software and libraries have been introduced, one of which is OpenFOAM, written in C++.

Given that toolbox refers to a container for keeping various tools in it, programming packages have a variety of tools called "toolbox. Programming toolboxes are written in different programming languages for different applications. Since C++ is a high-level, object-oriented, compiler, and fully-fledged programming language, it has gained popularity among programmers. Also, with the existing old packages, a large number of software developers use them. Because OpenFOAM is equipped with different tools for discretization, mesh generation, boundary conditions, and algorithms, it is known as a robust toolbox among the CFD community. OpenFOAM has taken advantage of the exceptional features of C++, especially object-oriented to create dynamical libraries and then, by using an interface called solver, connect the dynamical libraries to cases. OpenFoam' solvers are programs written for different conditions and problems. For instance, while `simpleFoam` solver possesses the ability to solve the forced convection, incompressible, and steady state problems, `pimpleFoam` or `pisoFoam` are used for aforementioned conditions but for transient problems. In the final step, by creating

cases including meshes, boundary conditions, properties, the studied problem can be solved. Since the first version of OpenFoam was released in 2004, only four toolboxes have been programmed and proposed. Wave generation toolbox was programmed by Jacobsen et al. [25] for simulation of wave propagation and wave breaking. Moreover, Elsafti and Oumeraci [26] developed a Foam toolbox for soil-structure interaction around marine structures. Also, Horgue et al. [27] designed `porousMultiphaseFoam` for modeling a multiphase flow in porous media. Finally, Cardiff et al. [23] programed a strong toolbox titled `solids4Foam` for simulation of solid-fluid interaction problems based on FVM for solid and fluid with various mathematical models for Fluid-Solid Coupling, mechanical laws, and dynamic meshes.

Unlike the OpenFOAM, the properties of a solid, liquid, or gaseous substance can be temperature-dependent. Moreover, this toolbox can get the materials of the core and shell of a M/N-EPCM from the user and generate it. Furthermore, the user is able to not only produce mono or hybrid nanofluids but also choose appropriate thermal conductivity and dynamic viscosity models among numerous previously provided models. Also, user can choose to solve the problem with homogenous or non-homogenous model (Buongiorno two-phase model) by choosing provided thermophoresis diffusion models. All these actions are done in `nanoFluid4Foam` libraries. Another characteristic of this library is that there are temperature-dependent and constant properties for different nanoparticles, base fluids, and PCMs. Hence, the users are no longer required to enter the properties while users have the opportunity to assign their desired substance's properties in `materials.H` file. The structure of the toolbox is shown in Figs. 1 and 2. According to Fig. 1, the toolbox is comprised of three main parts: `src4NF`, `applications4NF`, and `tutorials4NF`. Libraries are incorporated in `src4NF`, and the `applications4NF` and `tutorials4NF` have solvers and cases, respectively. In Fig. 2,

important toolbox libraries to generate nanoparticles, base fluids, mono and hybrid nanofluid are depicted.

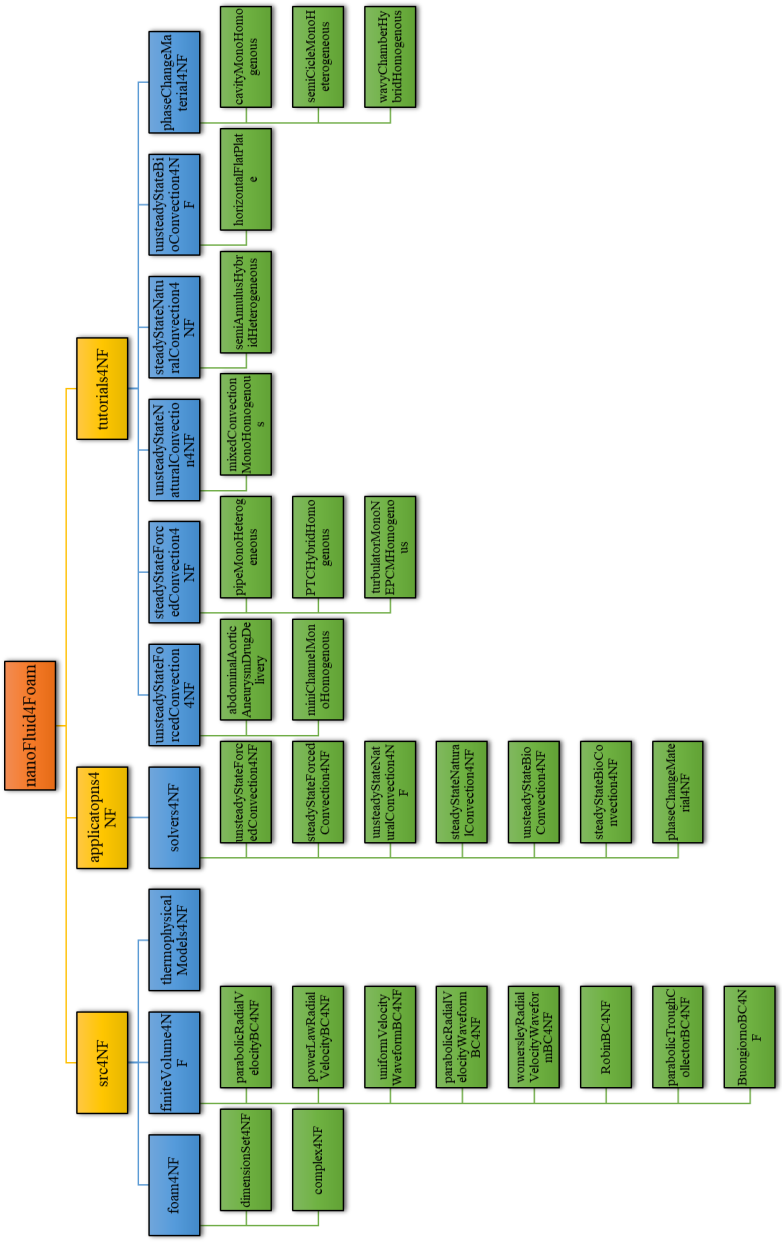

Figure 1. The structure of nanoFluid4Foam toolbox for libraries, solvers, and tutorials.

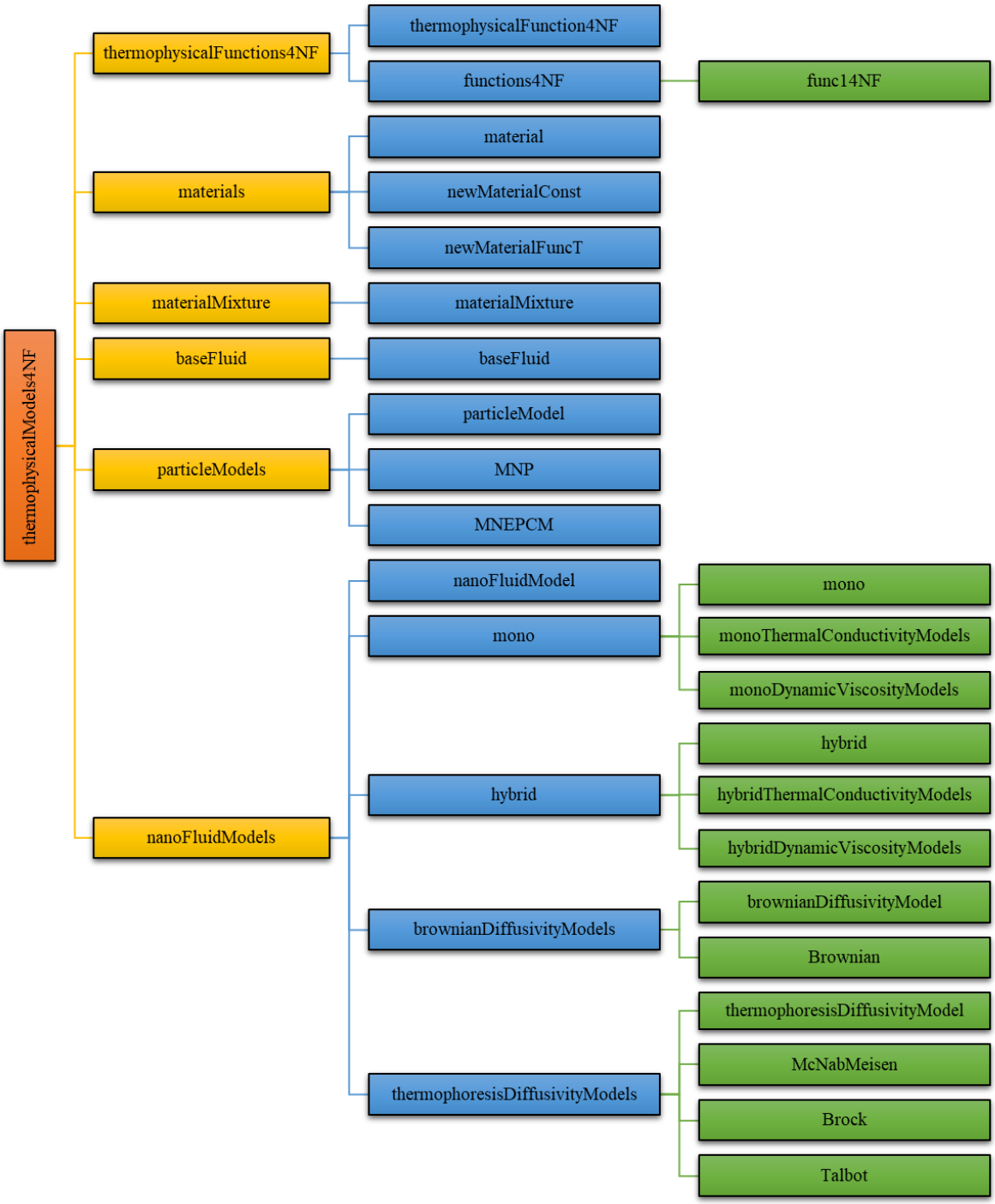

Figure 2. The structure of `thermophysicalProperties4NF` libraries.

3. API guide of nanoFluid4Foam toolbox

The heart of the nanoFluid4Foam toolbox is the `src4NF` library, containing a collection of classes. First, we investigate nanoFluid4Foam classes from the lowest (`thermophysicalFunction4NF`) to the highest-level class (`nanoFluidModel`). According to Figure 3, `thermophysicalFunction4NF` is a base class designed for functions depending on a variable; and derived class named NFFunc1 has inherited from it. Also, the material base class containing two derived classes called `newMaterialConst` and `newMaterialFuncT` (inherited from `thermophysicalFunction4NF`), which is used to compute the properties of a material as a function of temperature. In addition, the `materialMixture` is a documented class employed to calculate the combination of multi material to make a new material. It is worth mentioning that the aforementioned classes return just a scalar value. `baseFluid` class, a documented class, uses `materialMixture` class to create a material for base fluid. Moreover, `particleModel` class, a base class, is used to make solid and EPCM particles by derived classes named `MNP` and `MNEPCM` using `materialMixture` class.

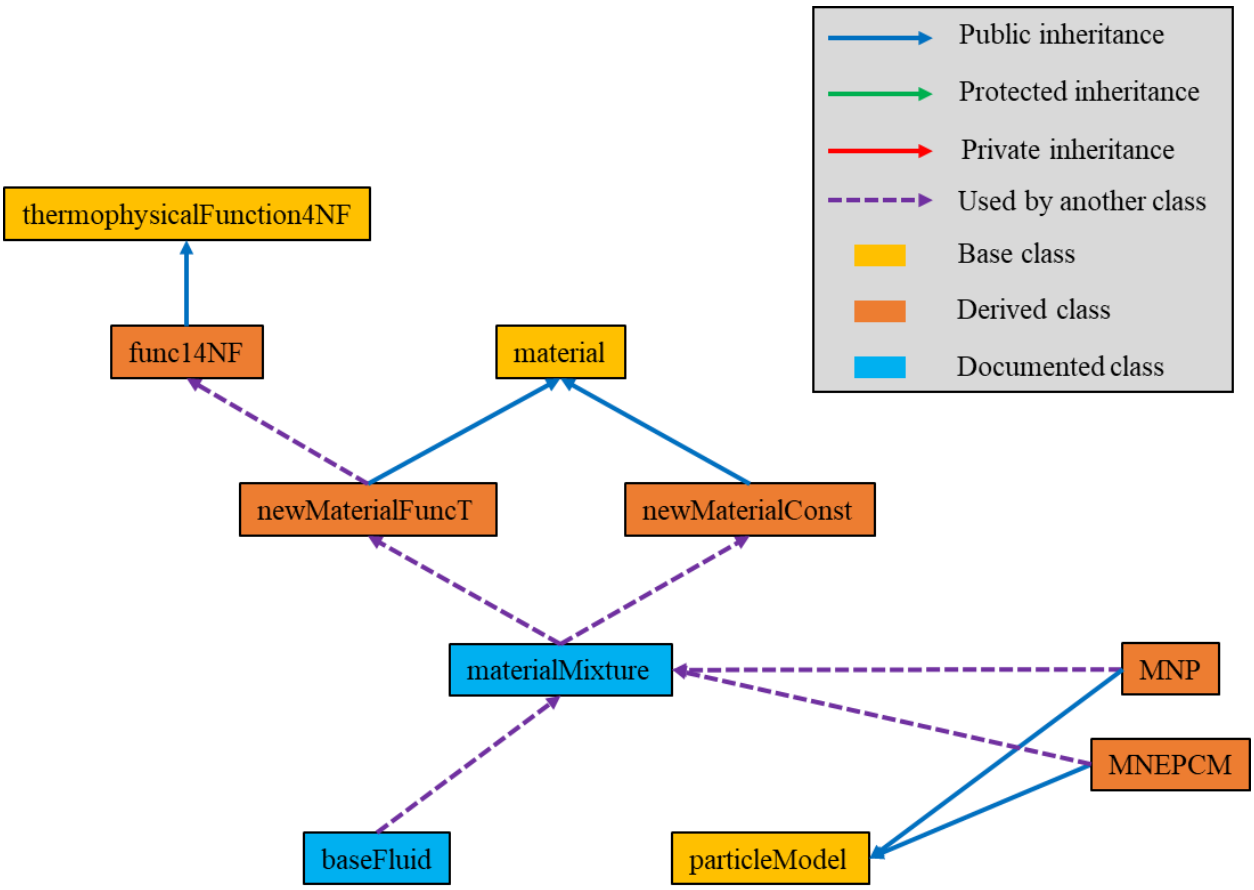

Figure 3. The API guide of nanoFluid4Foam toolbox from `thermophysicalFunction4NF` class to `baseFluid` and `particleModel` classes.

After maker classes for base fluid and particles, `nanoFluidModel` class, a base and documented class, is used to combine particles with base fluid to create a mono or hybrid nanofluids (derived classes) named by `mono` and `hybrid` (see Figure 4). Both `mono` and `hybrid` classes use linear relationships to compute density, specific heat capacity, and thermal expansion of nanofluid, whereas they have different models for thermal conductivity and dynamic viscosity of nanofluids. Two base classes named `monoThermalConductivityModel` and `monoDynamicViscosityModel` are made for different models for thermal conductivity and dynamic viscosity of mono nanofluid, and the models' names are shown in Figure 5. Also, two base classes named `hybridThermalConductivityModel` and

`hybridDynamicViscosityModel` are able to active various models (see Figure 6) for thermal conductivity and dynamic viscosity of hybrid nanofluid. Finally, a class with one model was made for Brownian diffusivity of particles, named `brownianDiffusivityModel`. In addition, three models for thermophoresis diffusivity were implanted, and the base class for it was named `thermophoresisDiffusivityModel.`

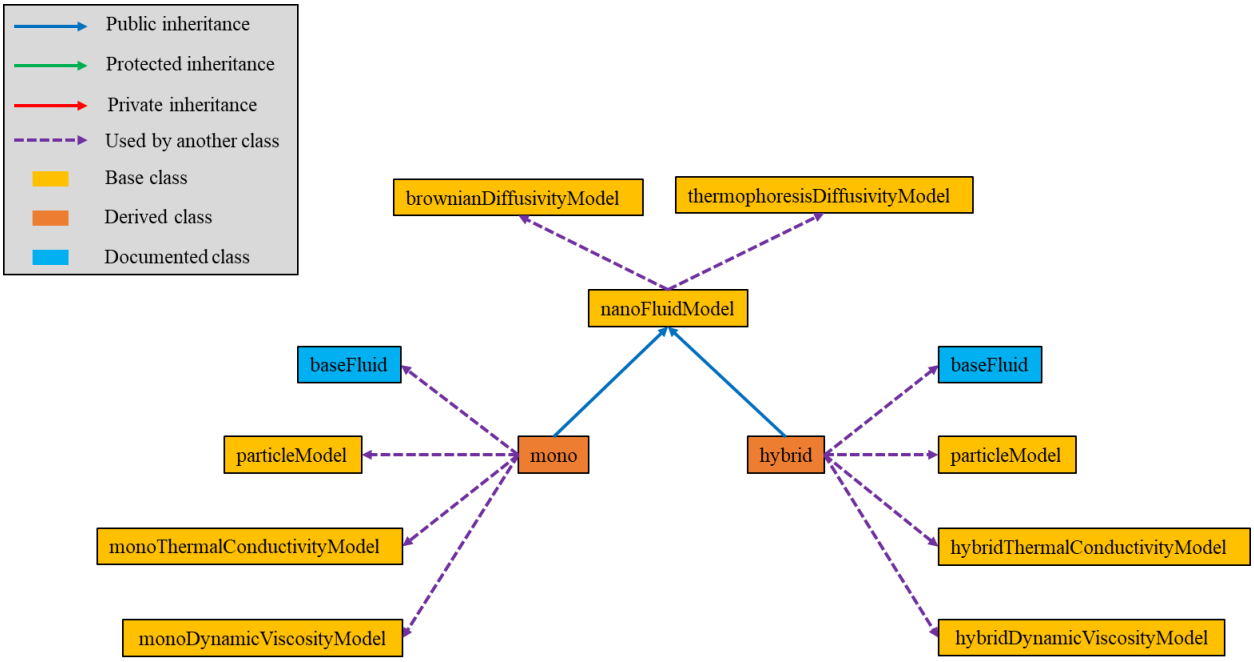

Figure 4. The API guide of nanoFluid4Foam toolbox for `nanoFluidModel` class.

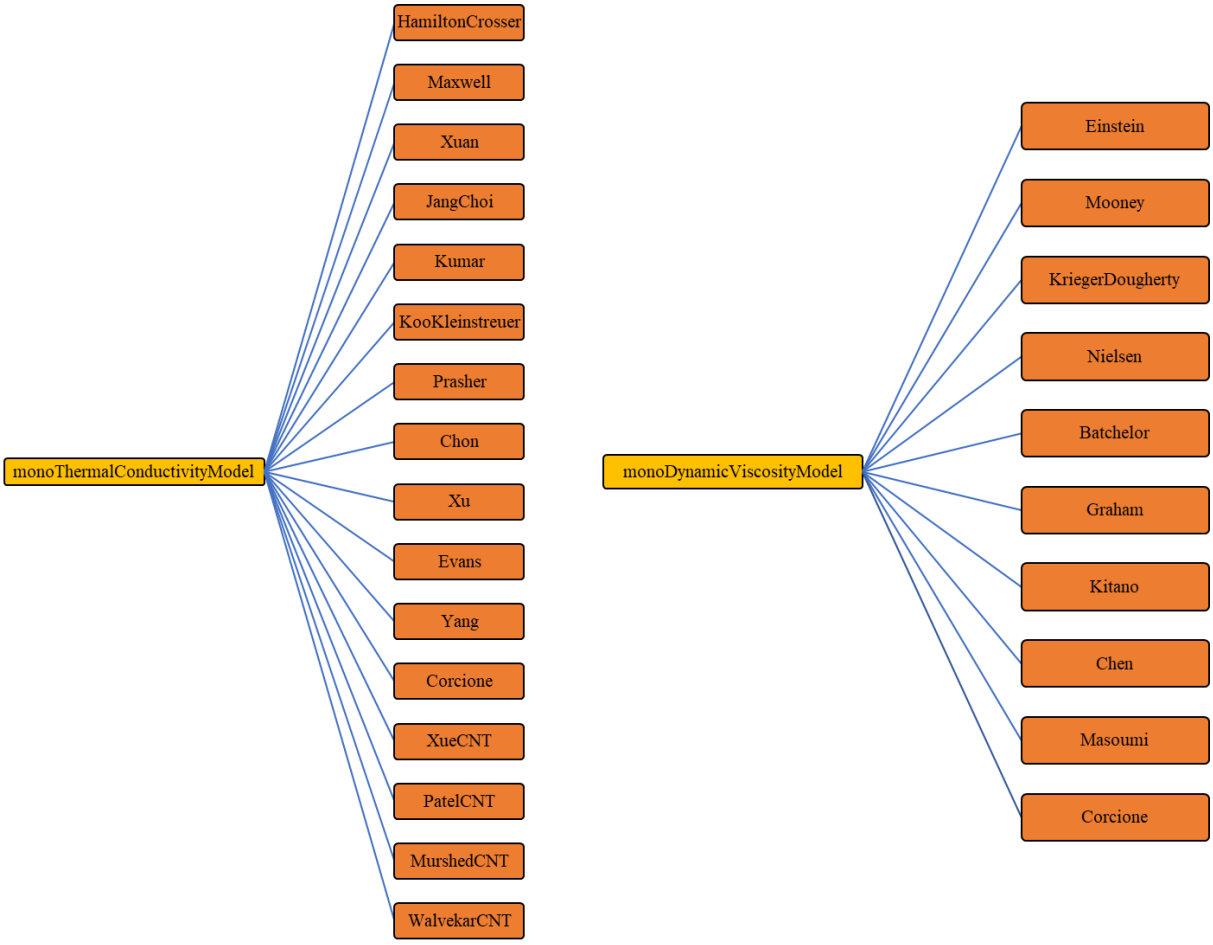

Figure 5. The API guide of nanoFluid4Foam toolbox for `monoThermalConductivityModel` and `monoDynamicViscosityModel` classes.

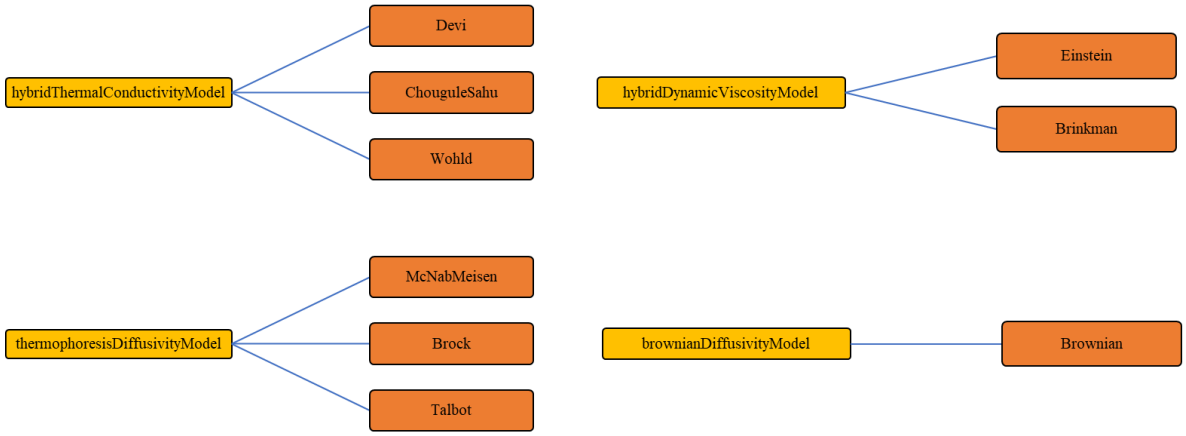

Figure 6. The API guide of nanoFluid4Foam toolbox for `hybridThermalConductivityModel`, `hybridDynamicViscosityModel`, `thermophoresisDiffusivityModel`, and `brownianDiffusivityModel` classes.

4. Mathematical models

This toolbox is able to use three types of particles, including solid, EPCM, and CNT (see Figure 7). The solid and CNT particles have a specific value for thermophysical properties, whereas the EPCM particle's equivalent thermophysical properties must be calculated with respect to the properties of the shell and core, so the current toolbox is capable of computing them according to the formulas listed in Table 1 for density, specific heat capacity, thermal conductivity, and thermal expansion.

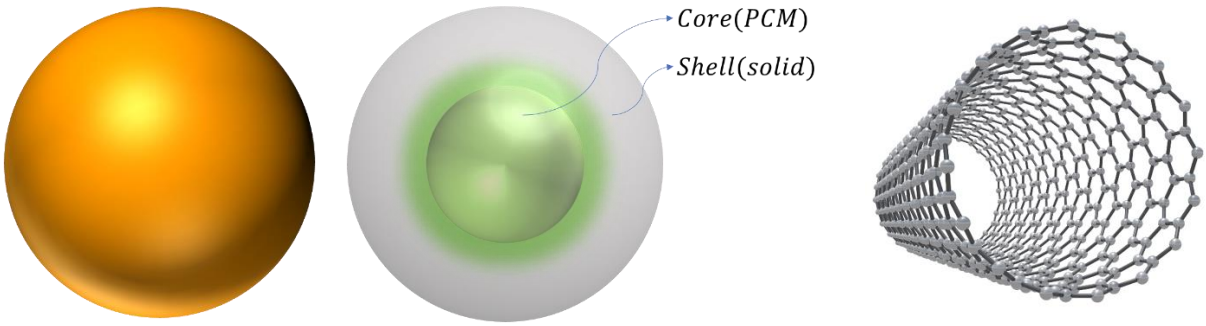

Figure 7. Three types of particle implementing in present toolbox.

According to Table 1, the density is calculated by taking into consideration the density of shell and core as well as an essential parameter known mass ratio of core to shell (ω). In addition, calculation of $C_{p,p}$ is the same as the calculation of ρ_p that uses density and specific heat capacity of shell and core and considers phase change process inside the core as a sinusoidal function of temperature. Moreover, effective thermal conductivity based on a multi-layer sphere

is considered to calculate the k_p with a spherical core and shell. Finally, Golab et al. [28] have proven a model for effective thermal expansion of EPCM depending on density and thermal expansion of the core and shell.

Table 1 Thermophysical properties of Nano/Micro-EPCM.

Properties	Formula
ρ_p	$\frac{(1+\omega)\rho_c\rho_s}{\rho_s+\omega\rho_c}$
$C_{p,p}$	$\frac{(C_{p,c}+\omega C_s)\rho_c\rho_s}{(\rho_s+\omega\rho_c)\rho_p}$ $C_{p,c}=C_{p,cl}+\left\{\frac{\pi}{2}\left(\frac{h_{fus}}{T_{Mr}}-C_{p,c\,l}\right)\left(\sin\pi\frac{T-\left(T_f-{T_{Mr}}/{2}\right)}{T_{Mr}}\right)\right\}\times\begin{cases}0\ if & T<T_f-\frac{T_{Mr}}{2}\\ 1\ if\ T_f-\frac{T_{Mr}}{2}<T<T_f+\frac{T_{Mr}}{2} & \\ 0\ if & T<T_f+\frac{T_{Mr}}{2}\end{cases}$
k_p	$\frac{d_s}{\frac{d_c}{k_c}+\frac{d_s-d_c}{k_s}}$ $d_c=d_s\left(\frac{\rho_s}{\rho_s+\omega\rho_c}\right)^{1/3}$
β_p	$\beta_c+\left(\frac{\beta_s-\beta_c}{2}\right)\left(\frac{1-\omega\rho_s}{\rho_c}\right)$

Needless to say, the thermophysical properties of particles affect that of nanofluid, and Table 2 arranged the density, specific heat capacity, and thermal expansion of mono and hybrid nanofluid, but there are different models for their thermal conductivity and dynamic viscosity.

Table 2 The thermophysical properties of mono and hybrid nanofluid.

Properties	Mono nanofluid	Hybrid nanofluid
ρ_{nf}	$(1-\varphi)\rho_{bf}+\rho_p\varphi$	$(1-\varphi_t)\rho_{bf}+\sum_{i=1}^{i=N}\rho_{p,i}\varphi_i$
$C_{p,nf}$	$\frac{(1-\varphi)\rho_{bf}C_{p,bf}+\rho_pC_{p,p}\varphi}{\rho_{mnf}}$	$\frac{(1-\varphi_t)\rho_{bf}C_{p,bf}+\sum_{i=1}^{i=N}\rho_{p,i}C_{p,p,i}\varphi_i}{\rho_{hnf}}$
k_{nf}	Table 3	Table 5

μ_{nf}	Table 4	Table 6
β_{nf}	$\frac{(1-\varphi)\rho_{bf}\beta_{bf}+\rho_p\beta_p\varphi}{\rho_{mnf}}$	$\frac{(1-\varphi_t)\rho_{bf}\beta_{bf}+\sum_{i=1}^{i=N}\rho_{p,i}\beta_{p,i}\varphi_i}{\rho_{hnf}}$

A variety of thermal conductivity models have been presented for mono nanofluid based on theory and semi-theory considering Brownian motion and convective heat transfer between base fluid and particles; well-known models are arranged in Table 3.

Table 3 The thermal conductivity of mono nanofluid (k_{mnf}).

Num.	Formula	Model name in `nanoFluid4Foam`	Ref.
1	$\frac{k_p+(\lambda-1)k_{bf}-(\lambda-1)(k_{bf}-k_p)\varphi}{k_p+(\lambda-1)k_{bf}+(k_{bf}-k_p)\varphi}k_{bf}$	HamiltonCrosser	[29]
2	$\frac{k_p+2k_{bf}-2(k_{bf}-k_p)\varphi}{k_p+2k_{bf}+(k_{bf}-k_p)\varphi}k_{bf}$	Maxwell	[30]
3	$\frac{k_p+2k_{bf}-2(k_{bf}-k_p)\varphi}{k_p+2k_{bf}+(k_{bf}-k_p)\varphi}k_{bf}+\rho_pC_p\varphi\sqrt{\frac{K_BT}{6\pi\mu_{bf}d_p}}$	Xuan	[31]
4	$(1-\varphi)k_{bf}+\beta\varphi k_p+C\frac{d_{bf}}{d_p}k_{bf}Re_p^2Pr_{bf}\varphi$ $\beta=0.01, C=18\times10^6, Re_p=\frac{\rho_{bf}\bar{C}_{R.M.}d_p}{\mu_{bf}}, \bar{C}_{R.M.}=\frac{K_BT}{3\pi\mu_{bf}d_pl_{bf}}, Pr_{bf}=\frac{C_{p,bf}\mu_{bf}}{k_{bf}}$	JangChoi	[32]
5	$k_{bf}+C_{c0}\bar{u}_p\frac{\varphi d_{bf}}{(1-\varphi)d_{bf}}$ $\bar{u}_p=\sqrt{\frac{2K_BT}{\pi\mu_{bf}d_p^2}}$	Kumar	[33]
6	$\frac{k_p+2k_{bf}-2(k_{bf}-k_p)\varphi}{k_p+2k_{bf}+(k_{bf}-k_p)\varphi}k_{bf}+5\times10^4\beta\varphi\rho_{bf}C_{p,bf}\sqrt{\frac{K_BT}{\rho_pd_p}}f(T,\varphi,etc.)$ $\beta=A_\beta(100\varphi)^{B_\beta}, f(T,\varphi)=(A_f\varphi+B_f)T+(C_f\varphi+D_f)$	KooKleinstreuer	[34]
7	$\left(1+ARe_p^MPr_{bf}^{1/3}Pr_{bf}\varphi\right)\left[\frac{k_p+2k_{bf}-2(k_{bf}-k_p)\varphi}{k_p+2k_{bf}+(k_{bf}-k_p)\varphi}\right]k_{bf}$	Prasher	[35]

	$A = 4 \times 10^4, Re_p = \frac{\rho_{bf}}{\mu_{bf}}\sqrt{\frac{18K_BT}{\pi\rho_p d_p}}, Pr_{bf} = \frac{C_{p,bf}\mu_{bf}}{k_{bf}}$		
8	$\left(1 + 64.7\varphi^{0.746}\left(\frac{d_{bf}}{d_p}\right)^{0.369}\left(\frac{k_p}{k_{bf}}\right)^{0.369} Re_p^{1.2321} Pr_{bf}^{0.9955}\right)k_{bf}$ $Re_p = \frac{\rho_{bf}K_BT}{3\pi\mu_{bf}^2 l_{bf}}, Pr_{bf} = \frac{C_{p,bf}\mu_{bf}}{k_{bf}}$	Chon	[36]
9	$\frac{k_p + 2k_{bf} - 2(k_{bf} - k_p)\varphi}{k_p + 2k_{bf} + (k_{bf} - k_p)\varphi}k_{bf} + H\frac{Nu_p d_{bf}}{Pr_{bf}}\frac{(2-D)D}{(1-D)^2}\frac{\left[\left(\frac{d_{max}}{d_{min}}\right)^{1-D} - 1\right]^2}{\left[\left(\frac{d_{max}}{d_{min}}\right)^{2-D} - 1\right]}\frac{k_{bf}}{\bar{d}_p}$ $D = d - \left[\frac{Ln\,\varphi}{Ln\left(\frac{d_{min}}{d_{max}}\right)}\right], Pr_{bf} = \frac{C_{p,bf}\mu_{bf}}{k_{bf}}$	Xu	[37]
10	$\left(1 + 3\varphi\frac{\gamma - 1}{\gamma + 2}\right)k_{bf}$	Evans	[38]
11	$\left[1 + 3\varphi\frac{\frac{d_p}{2R_b k_{bf}} - 1}{\frac{d_p}{2R_b k_{bf}} + 2}\right]k_{bf} + 157.5\varphi C_{p,bf}u_p^2\tau_p$ $u_p = \sqrt{\frac{3K_BT}{m_p}}, \tau_p = \frac{m_p}{3\pi\mu_{bf}d_p}$	Yang	[39]
12	$\left(1 + 4.4Re_p^{0.4}Pr_{bf}^{0.66}\varphi^{0.66}\left(\frac{T}{T_{fr}}\right)^{10}\left(\frac{k_p}{k_{bf}}\right)^{0.03}\right)k_{bf}$ $Re_p = \frac{2\rho_{bf}K_BT}{\pi\mu_{bf}^2 d_p}, Pr_{bf} = \frac{C_{p,bf}\mu_{bf}}{k_{bf}}$	Corcione	[40]
13	$\frac{3 + \varphi(\beta_{11} + \beta_{33})}{3 - \varphi\beta_{11}}k_{bf}$ $\beta_{11} = \frac{2(k_{11}^c - k_{bf})}{k_{11}^c + k_{bf}}, \beta_{33} = \frac{k_{33}^c}{k_{bf}} - 1$ $k_{11}^c = \frac{k_p}{1 + \frac{2a_k k_p}{d_{CNT}k_{bf}}}, k_{33}^c = \frac{k_p}{1 + \frac{2a_k k_p}{L_{CNT}k_{bf}}}$ $a_k = R_k k_{bf}, R_k = 8 \times 10^{-8}$	NanCNTC	[41]
14	$\frac{1 - \varphi + 2\varphi\frac{k_p}{k_p - k_{bf}}Ln\frac{k_p + k_{bf}}{2k_{bf}}}{1 - \varphi + 2\varphi\frac{k_{bf}}{k_p - k_{bf}}Ln\frac{k_p + k_{bf}}{2k_{bf}}}k_{bf}$	XueCNT	[42]
15	$\left[1 + \frac{k_p\varphi d_{bf}}{k_{bf}(1-\varphi)d_{CNT}}\right]k_{bf}$	PatelCNT	[43]

16	$\frac{(k_p - k_{lr})(\gamma_1^2 - \gamma^2 + 1)\varphi k_{lr} + (k_p + k_{lr})[\varphi\gamma^2(k_{lr} - k_{bf}) + k_{bf}]\gamma_1^2}{\gamma_1^2(k_p + k_{lr}) - (k_p - k_{lr})(\gamma_1^2 + \gamma^2 - 1)\varphi}$ $k_{lr} = C_{lr}k_{bf}, \gamma_1 = 1 + \frac{2t}{d_{CNT}}, \gamma = 1 + \frac{t}{d_{CNT}}, t = \sigma\sqrt{2\pi}$	MurshedCNT	[44]
17	$\left[1 + \frac{k_p \frac{\varphi(d_{CNT} + 2L_{CNT})}{d_{CNT}L_{CNT}}}{k_{bf}\frac{3(1-\varphi)}{d_{bf}}}\right]k_{bf} + \frac{4C\varphi(T - T_0)}{d_{CNT}^2 L_{CNT}^2 \mu_{bf}} Ln\left(\frac{L_{CNT}}{d_{CNT}}\right)$ $C = \frac{84K_B^2}{72\pi^2}$	WalvekarCNT	[45]

Also, different dynamic viscosity models for mono nanofluid have been proposed considering particle concentration and particle clotting inside base fluid. Table 4 lists some prominent models for the dynamic viscosity of mono nanofluids. 4.

Table 4 The dynamic viscosity of mono nanofluid (μ_{mnf}).

Num.	Formula	Model name in `nanoFluid4Foam`	Ref.
1	$(1 + 2.5\varphi)\mu_{bf}$	Einstein	[46]
2	$\mu_{bf}e^{\left(\frac{\xi\varphi}{1-k\varphi}\right)}$	Mooney	[47]
3	$\mu_{bf}\left[1 - \frac{\varphi}{\varphi_m}\right]^{-\eta\varphi_m}$	KriegerDougherty	[48]
4	$\mu_{bf}(1 + 2.5\varphi)e^{\left(\frac{\varphi}{1-\varphi_m}\right)}$	Nielsen	[49]
5	$(1 + 2.5\varphi + 6.5\varphi^2)\mu_{bf}$	Batchelor	[50]
6	$\frac{\mu_{bf}}{(1-\varphi)^{2.5}}$	Brinkman	[51]
7	$\mu_{bf}\left(1 + 2.5\varphi + 4.5\left[\frac{1}{\left(\frac{h}{d_p}\left(2 + \frac{h}{d_p}\right)\right)\left(1 + \frac{h}{d_p}\right)^2}\right]\right)$	Graham	[52]
8	$\frac{\mu_{bf}}{\left[1 - \frac{\varphi}{\varphi_m}\right]^2}$	Kitano	[53]
9	$\mu_{bf}\left(1 - \frac{\varphi_a}{\varphi_m}\right)^{-2.5\varphi_m}$ $\varphi_a = \varphi\left(\frac{a_a}{a}\right)^{3-D}$	Chen	[54]

10	$\mu_{bf}\left(1+\frac{\rho_p u_B d_p^2}{72C\delta\mu_{bf}}\right)$ $u_B=\frac{1}{d_p}\sqrt{\frac{18K_BT}{\pi\rho_p d_p}}, \delta=d_p\left(\frac{\pi}{6\varphi}\right)^{1/3}, C=\frac{1}{\mu_{bf}}\left((c_1d_p+c_2)\varphi+(c_3d_p+c_4)\right)$	Masoumi	[55]
11	$\mu_{bf}\left(\frac{1}{1-34.87\left(\frac{d_p}{d_{bf}}\right)^{-0.3}\varphi^{1.03}}\right)$	Corcione	[56]

Given the novelty of hybrid nanofluid, only a few models for its thermal conductivity and dynamic viscosity have been proposed; however, many researchers have developed mono nanofluid models for hybrid nanofluid, as shown in Tables 5 and 6.

Table 5 The thermal conductivity of hybrid nanofluid (k_{hnf}).

Num.	Formula	Model name in `nanoFluid4Foam`	Ref.
1	$k_{bf}\prod_{i=1}^{i=N}\frac{k_{p,i}+(\lambda_i-1)k_{bf}-(\lambda_i-1)(k_{bf}-k_{p,i})\varphi_i}{k_{p,i}+(\lambda_i-1)k_{bf}+(k_{bf}-k_{p,i})\varphi_i}$	Devi	[57]
2	$k_{bf}\left[1+\sum_{i=1}^{i=N}\frac{k_{p,i}\varphi_i d_{bf}}{k_{bf}(1-\varphi_t)d_{p,i}}\right]$ $\varphi_t=\sum_{i=1}^{i=N}\varphi_i$	ChouguleSahu	[58]
3	$k_{bf}\prod_{i=1}^{i=N}\left[1+0.135\left(\frac{k_{p,i}}{k_{hnf,i-1}}\right)^{0.273}\left(\frac{T}{20}\right)^{0.547}\left(\frac{100}{d_{p,i}}\right)^{0.234}\varphi_i^{0.467}\right]$	Wohld	[59]

Table 6 The dynamic viscosity of hybrid nanofluid (μ_{hnf}).

Num.	Formula	Model name in `nanoFluid4Foam`	Ref.
1	$(1+2.5\varphi_t)\mu_{bf}$ $\varphi_t=\sum_{i=1}^{i=N}\varphi_i$	Einstein	[60]

2	$\frac{\mu_{bf}}{\prod_{i=1}^{i=N}(1-\varphi_i)^{2.5}}$	Brinkman	[61]

As mentioned before, the famous Buongiorno model was implemented in the current toolbox, including one model for Brownian diffusivity and three models for thermophoresis diffusivity according to Tables 7 and 8.

Table 7 The Brownian diffusivity (D_B).

Num.	Formula	Model name in `nanoFluid4Foam`	Ref.
1	$\frac{K_B T}{3\pi\mu_{bf} d_p}$	Brownian	[62]

Table 8 The constant parameter (β_T) of thermophoresis diffusivity ($D_T = \beta_T \frac{\mu_{bf}}{\rho_{bf}}\varphi$).

Num.	Formula	Model name in `nanoFluid4Foam`	Ref.
1	$0.26\frac{k_{bf}}{2k_{bf}+k_p}$	McNabMeisen	[63]
2	$\frac{2C_s(k_{bf}+k_pKn)}{(1+3C_mKn)(2k_{bf}+k_p+2k_pC_tKn)}$ $Kn=\frac{l_{bf}}{d_p}$	Brock	[64]
3	$\frac{2C_s(k_{bf}+k_pKn)\left[1+Kn\left(1.2+0.41e^{-0.88/Kn}\right)\right]}{(1+3C_mKn)(2k_{bf}+k_p+2k_pC_tKn)}$ $Kn=\frac{l_{bf}}{d_p}$	Talbot	[65]

5. Solvers

In this toolbox, four solvers (see Figure 1) were programmed to use new library for forced and natural convection, and also for steady and unsteady states. Moreover, a new PDE equation was

programmed to compute concentration based on Brownian and thermophoresis diffusions. Hence, the governing equations including mass, momentum, energy, and concentration conservations are following [70] and [71]:

$$\nabla.\left(\rho_{nf}\vec{V}\right)=0 \tag{1-1}$$

$$\frac{\partial\left(\rho_{nf}\vec{V}\right)}{\partial t}+\nabla.\left(\rho_{nf}\vec{V}\vec{V}\right)=-\nabla P+\nabla.\left(\mu_{nf}\nabla\vec{V}\right)+S_{m,Tb} \tag{1-2}$$

$$S_{m,Tb}=\rho_{nf}\vec{g}\beta_{nf}\left(T-T_{ref}\right) \tag{1-3}$$

$$\frac{\partial\left(\rho_{nf}C_{p,nf}T\right)}{\partial t}+\nabla.\left(\rho_{nf}C_{p,nf}T\vec{V}\right)=\nabla.\left(k_{nf}\nabla T\right)+\sum_{i=1}^{i=N}S_{e,p,i} \tag{1-4}$$

$$S_{e,p,i}=\rho_{p,i}C_{p,p,i}\nabla T.\left(D_{B,i}\nabla\varphi_i+D_{T,i}\frac{\nabla \mathrm{T}}{T}\right) \tag{1-5}$$

$$\frac{\partial\varphi_i}{\partial t}+\nabla.\left(\varphi_i\vec{V}\right)=\nabla.\left(D_{B,i}\nabla\varphi_i+D_{T,i}\frac{\nabla \mathrm{T}}{T}\right) \tag{1-6}$$

The temporal term (first term in left hand) is omitted in steady state, and Buoyant force (Eq.1-3) is removed in forced convection solvers. Also, concentration equation (1-6) is not solved in homogenous assumption.

In addition, A new solver was programmed for phase change material based on the enthalpy-porosity method extended by a continuous enthalpy function without updating. But, an error function was embedded to calculate liquid fraction in iterative, which is coupled by energy conservation to be updated [72]. Therefore, mass, momentum, energy, and concentration equations conservation are arranged as below:

$$\nabla.\left(\rho_{nf}\vec{V}\right)=0 \tag{2-1}$$

$$\frac{\partial\left(\rho_{nf}\vec{V}\right)}{\partial t}+\nabla.\left(\rho_{nf}\vec{V}\vec{V}\right)=-\nabla P+\nabla.\left(\mu_{nf}\nabla\vec{V}\right)+S_{m,Tb}+S_{m,pcm} \tag{2-2}$$

$$S_{m,Tb}=\rho_{nf}\vec{g}\beta_{nf}\left(T-T_{ref}\right) \tag{2-3}$$

$$S_{m,pcm}=-C\frac{(1-\gamma)^2}{\gamma^3+b}\vec{V} \tag{2-4}$$

$$\frac{\partial(\rho_{nf}C_{p,nf}T)}{\partial t}+\nabla.(\rho_{nf}C_{p,nf}T\vec{V})=\nabla.(k_{nf}\nabla T)+S_{e,pcm}+\sum_{i=1}^{i=N}S_{e,p,i} \quad (2\text{-}5)$$

$$S_{e,pcm}=-h_f\left(\frac{\partial(\rho_{nf}\gamma)}{\partial t}+\nabla.(\rho_{nf}\gamma\vec{V})\right) \quad (2\text{-}6)$$

$$S_{e,p,i}=\rho_{p,i}C_{p,p,i}\nabla T.\left(D_{B,i}\nabla\varphi_i+D_{T,i}\frac{\nabla \mathrm{T}}{T}\right) \quad (2\text{-}7)$$

$$\gamma=0.5\,erf\left(4\frac{T_s-T_f}{T_l-T_s}\right)+0.5 \quad (2\text{-}8)$$

$$\frac{\partial\varphi_i}{\partial t}+\nabla.(\varphi_i\vec{V})=\nabla.\left(D_{B,i}\nabla\varphi_i+D_{T,i}\frac{\nabla \mathrm{T}}{T}\right) \quad (2\text{-}9)$$

Moreover, another solver was embedded for bioconvection problems consisting of a base fluid, mono or hybrid nanoparticle, and microorganism. In momentum equations, three Buoyant forces due to density change by fluid temperature, nanoparticle concentration, and microorganism concentration. Also, an activation energy was added to nanoparticle concentration. So, mass, momentum, energy, nanoparticle, and microorganism concentrations conservation are following [73-75]:

$$\nabla.(\rho_{nf}\vec{V})=0 \quad (3\text{-}1)$$

$$\frac{\partial(\rho_{nf}\vec{V})}{\partial t}+\nabla.(\rho_{nf}\vec{V}\vec{V})=-\nabla P+\nabla.(\mu_{nf}\nabla\vec{V})+S_{m,Tb}+S_{m,mb}+\sum_{i=1}^{i=N}S_{m,Cb,i} \quad (3\text{-}2)$$

$$S_{m,Tb}=-\rho_{bf}\vec{g}\beta_{bf}(1-\varphi_t)(T-T_{ref}) \quad (3\text{-}3)$$

$$S_{m,Cb,i}=\vec{g}\beta_{\varphi_i}(\rho_{p,i}-\rho_{bf})(\varphi_i-\varphi_{ref,i}) \quad (3\text{-}4)$$

$$S_{m,mb}=\vec{g}\beta_n(\rho_o-\rho_{bf})(n-n_{ref}) \quad (3\text{-}5)$$

$$\frac{\partial(\rho_{nf}C_{p,nf}T)}{\partial t}+\nabla.(\rho_{nf}C_{p,nf}T\vec{V})=\nabla.(k_{nf}\nabla T)+\sum_{i=1}^{i=N}S_{e,p,i} \quad (3\text{-}6)$$

$$S_{e,p,i}=\rho_{p,i}C_{p,p,i}\nabla T.\left(D_{B,i}\nabla\varphi_i+D_{T,i}\frac{\nabla \mathrm{T}}{T}\right) \quad (3\text{-}7)$$

$$\frac{\partial\varphi_i}{\partial t}+\nabla.(\varphi_i\vec{V})=\nabla.\left(D_{B,i}\nabla\varphi_i+D_{T,i}\frac{\nabla \mathrm{T}}{T}\right)+\sum_{i=1}^{i=N}S_{C,a,i} \quad (3\text{-}8)$$

$$S_{C,a,i}=-{k_{r,i}}^2(\varphi_i-\varphi_{ref,i})\left(\frac{T}{T_{ref}}\right)^{N_i}e^{\left(-\frac{E_{a,i}}{K_BT}\right)} \quad (3\text{-}9)$$

$$\frac{\partial n}{\partial t} + \nabla.\left(n\vec{V}\right) = \nabla.\left(D_{mo}\nabla n\right) - \sum_{i=1}^{i=N} \nabla.\left(\frac{Wbn}{\left(\varphi_i - \varphi_{ref}\right)}\nabla\varphi_i\right) \quad (3\text{-}10)$$

In all solvers, steady and unsteady states were implemented based on SIMPLE and PISO algorithms, respectively. Also, they are capable to solve laminar and turbulent problems according to OpenFoam instructions by setup model and requirement boundary conditions corresponding to selected turbulence model.

6. Boundary conditions

6.1. Velocity boundary conditions

Many boundary conditions were implemented for velocity, temperature, and concentration based on Dirichlet, Neumann, and Robin approaches for value, gradient, and mixed boundary conditions, respectively. A parabolic and a power law radial velocity were implemented for circle patches, which are used in laminar and turbulent boundary conditions in inlets, respectively. So, it was computed as following [19]:

$$V_x(r) = 2V_{avg}\left(1 - \left(\frac{r}{R}\right)^2\right) \quad (4)$$

$$V_x(r) = C_m V_{avg}\left(1 - \left(\frac{r}{R}\right)\right)^{1/m} \quad (5\text{-}1)$$

$$C_m = \frac{\left(1 + \frac{1}{m}\right)\left(2 + \frac{1}{m}\right)}{2} \quad (5\text{-}2)$$

Moreover, a uniform and parabolic waveform velocity for inlet patches were programmed, which is applicable for cardiovascular problems. Hence, they can calculate as following [76 and 77]:

$$V_x(t) = \sum_{n=0}^{n=+\infty} a_n cos(n\omega t) + b_n sin(n\omega t) \tag{6}$$

$$V_x(r,t) = 2\left(1 - \left(\frac{r}{R}\right)^2\right) \times \sum_{n=0}^{n=+\infty} a_n cos(n\omega t) + b_n sin(n\omega t) \tag{7}$$

Another important boundary in cardiovascular problems is Womersley for inlet patches, observed in periodic gradient pressure. Hence, it was computed as below [78]:

$$\frac{\partial p}{\partial x}(t,n) = \sum_{n=-\infty}^{n=+\infty} G_n e^{in\omega t} = \sum_{n=0}^{n=+\infty} G_n cos(n\omega t) + iG_n sin(n\omega t) \tag{8-1}$$

$$Wo = R\sqrt{\frac{\omega}{\nu}} \tag{8-2}$$

$$Wo_n = Wo\sqrt{n} \tag{8-3}$$

$$s_n = i^{\frac{3}{2}} Wo_n \tag{8-4}$$

$$\bar{V} = \frac{\omega}{2\pi} \int_0^{2\pi/\omega} V(t)\, dt \tag{8-5}$$

$$Re = \frac{2\bar{V}R}{\nu} \tag{8-6}$$

$$V_x(r,t) = \frac{ReG_0R^2}{8}\left(1 - \left(\frac{r}{R}\right)^2\right) + \frac{ReR^2}{i} \sum_{n=-\infty}^{n=+\infty} \frac{G_n}{Wo_n^2}\left[1 - \frac{J_0\left(s_n\left(\frac{r}{R}\right)\right)}{J_0(s_n)}\right] e^{in\omega t} \tag{8-7}$$

$$G_0 = \frac{4}{R^2 Re} V_0 \tag{8-8}$$

$$G_n = \frac{iWo_n^2}{2R^2 Re\left(1 - F(s_n)\right)} V_n \tag{8-9}$$

$$F(s_n) = \frac{2}{s_n}\frac{J_1(s_n)}{J_0(s_n)} \tag{8-10}$$

$$V_x(t,n) = \sum_{n=0}^{n=+\infty} a_n cos(n\omega t) + ib_n sin(n\omega t) \tag{8-11}$$

6.2. Temperature boundary conditions

For temperature boundary condition, some boundary conditions were added. A Robin boundary condition was programmed for wall patches, is calculated as bellow:

$$\nabla T = \frac{1}{k_{nf}}\left(q''(x) - h_o(T - T_o)\right) \quad (9\text{-}1)$$

$$q''(x) = \sum_{n=0}^{n=\infty} a_n x^n \quad (9\text{-}2)$$

In heat transfer process, non-uniform heat flux exposed to parabolic trough collector system is a most complicated and vital boundary condition is such systems. Hence, some equations and relationships need to be solved and calculated according to following [19]:

$$LCR_i(\theta) = \sum_{n=0}^{n=\infty} a_n \theta^n \quad (10\text{-}1)$$

$$\nabla T = \frac{1}{k_{nf}}\left(q''(\theta) - \frac{\dot{Q}_{t-g}}{A_t}\right) \quad (10\text{-}2)$$

$$q''(\theta) = I_s \tau_g \alpha_t LCR(\theta) \quad (10\text{-}3)$$

In order to calculate heat loss from absorber tube ($\dot{Q}_{t-g}$), a function (f_g) was solved based on bisection method according to following [19]:

$$\dot{Q}_{abs,g} = I_s \alpha_g \overline{LCR} A_g \quad (10\text{-}4)$$

$$A_g = 2\pi R_g L \quad (10\text{-}5)$$

$$\dot{Q}_{loss,g} = A_g h_a\left(\bar{T}_g - T_a\right) + A_g \varepsilon_g \sigma_{sb}\left({\bar{T}_g}^4 - {T_{sky}}^4\right) \quad (10\text{-}6)$$

$$T_{sky} = 0.0522 {T_a}^{1.5} \quad (10\text{-}7)$$

$$\dot{Q}_{t-g} = \frac{A_t \sigma_{sb}\left({T_t}^4 - {T_g}^4\right)}{\frac{1}{\varepsilon_t} + \frac{1-\varepsilon_g}{\varepsilon_g}\frac{R_t}{R_g}} \quad (10\text{-}8)$$

$$A_t = 2\pi R_t L \quad (10\text{-}9)$$

$$\bar{T}_t = \frac{\int_0^L \int_0^{2\pi} T_t R_t \, d\theta \, dx}{\int_0^L \int_0^{2\pi} R_t \, d\theta \, dx} \quad (10\text{-}10)$$

$$f_g = \dot{Q}_{t-g} - \left[\dot{Q}_{abs,g} - \dot{Q}_{loss,g}\right] \quad (10\text{-}11)$$

6.3. Concentration boundary conditions

Finally, a boundary condition (Robin) was programmed to concentration equation, appropriate for wall with zero velocity. So, it is calculated for each nanoparticle as following [15] and [71]:

$$\nabla\varphi_i = h_c(\varphi_i - \varphi_{amb}) - \frac{D_{T,i}}{D_{B,i}}\frac{\nabla \mathrm{T}}{T} \quad (11)$$

7. Validations

In order to assess the Buongiorno two-phase model and nanoparticles' distribution, a numerical study by Yekani et al. [66] was chosen. Yekani et al. [66] simulated natural convection heat transfer of alumina-water suspension in a square for various nanoparticles' volume fraction $0.01 \leq \varphi \leq 0.04$, inclination angles $0° \leq \theta \leq 60°$, and Rayleigh numbers $10^2 \leq Ra \leq 10^6$ in a cavity under these conditions: $L = 0.025\, m, \Delta T = 2\, K, Ra_f = 10^6, \varphi = 0.03, d_p = 33\, nm, and\ T_c = 298.0$. The left and right walls temperature were supposed to be constant and served as hot and cold walls, respectively. As can be seen in Fig. 8, the obtained volume fraction contours are faithful to those of Yekani.

Yekani et al. [66] Present

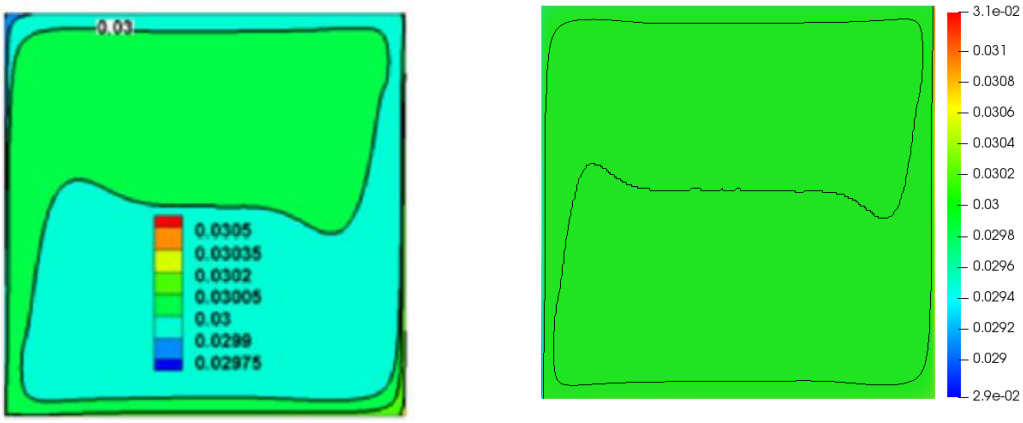

Heris et al. [67] experimentally investigated forced convection flow of a nanofluid comprised of water and alumina nano-sized particles in a tube with diameter 3mm and length 1m under constant wall temperature for different Peclet numbers ($2000 \leq Pe \leq 7000$) and nanoparticles' volume fractions ($0.002 \leq \varphi \leq 0.04$). The obtained average Nusselt number were compared with their findings, and a maximum difference percentage around 4% was observed which is acceptable.

Table 9 The average Nusselt number for Al_2O_3 for volume fraction of 0.2%.

Peclet	Exp.	Num.	Error (%)
3000	5.08	5.27	3.7
4500	5.95	5.78	2.8
6000	6.5	6.23	4.1

Kamkari et al. [68] experimentally scrutinized melting of lauric acid phase change material in an enclosure for different inclination angles, hot wall temperatures, and Rayleigh numbers. All walls were thermally insulated except one wall that was heated isothermally. Fig . depicts

comparison of melting fraction between the present study and Kamkari et al. [68]. As can be inferred from the Fig. 9, the results are consistent with each other.

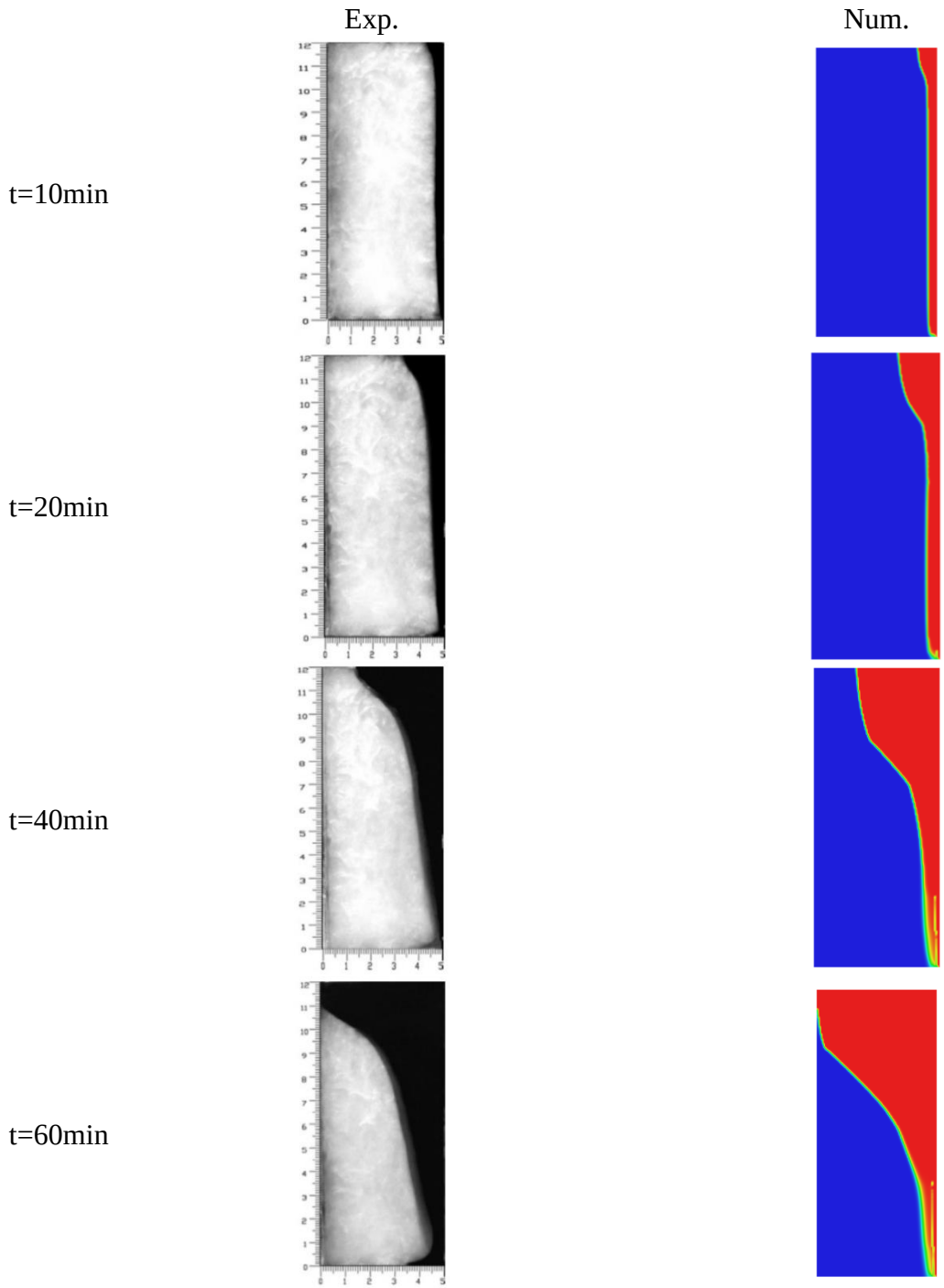

t=80min

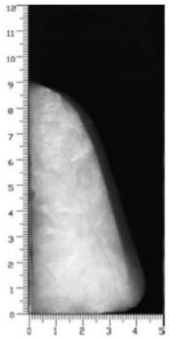

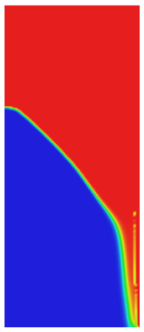

Fig. 9. Comparison of liquid fraction results of present numerical code with experimental photographs for different times for melting of lauric acid in an enclosure.

In order to verify natural convective heat transfer of nanofluids, a numerical study was chosen. Kahveci [69] numerically studied laminar flow of alumina nanoparticles-water in a cavity for different nanoparticles type, nanoparticles volume fractions $0 \leq \varphi \leq 0.2$, tilt angles $0° \leq \theta \leq 60°$, and Rayleigh numbers$10^4 \leq Ra \leq 10^6$. A comparison between the present study and Kahveci for average Nusselt number reveals that there is only a maximum deviation of 1.9 % confirming that the present written library is confidential for modeling.

Table 10 The average Nusselt number for Al_2O_3 for volume fraction of 5% and inclination angle of 0°.

Ra_{nf}	Kahvaci	Present study	Error (%)
10^4	2.37	2.40	1.3
10^5	4.97	5.02	1
10^6	9.78	9.97	1.9

References

[1] J. C. Maxwell, A Treatise on Electricity and Magnetism, Clarendon Press, Oxford, UK, 1891.

[2] S. U. S. Choi, Y. I. Cho, and K. E. Kasza, “Degradation effects of dilute polymer solutions on turbulent friction and heat transfer behavior,” Journal of Non-Newtonian Fluid Mechanics, vol. 41, no. 3, pp. 289–307, 1992.

[3] Angayarkanni, S.A. and Philip, J., 2015. Review on thermal properties of nanofluids: Recent developments. Advances in colloid and interface science, 225, pp.146-176.

[4] Y. Xuan and Q. Li, “Heat transfer enhancement of nanofluids,” International Journal of Heat and Fluid Flow, vol. 21, no. 1, pp. 58–64, 2000.

[5] Wong, K.V. and De Leon, O., 2010. Applications of nanofluids: current and future. Advances in mechanical engineering, 2, p.519659.

[6] H. Nazir, M. Batool, F. J. Bolivar Osorio et al., “Recent developments in phase change materials for energy storage applications: a review,” International Journal of Heat and Mass Transfer, vol. 129, pp. 491–523, 2019.

[7] K. Pielichowska and K. Pielichowski, “Phase change materials for thermal energy storage,” Progress in Materials Science, vol. 65, pp. 67–123, 2014.

[8] Peng, G., Dou, G., Hu, Y., Sun, Y. and Chen, Z., 2020. Phase change material (PCM) microcapsules for thermal energy storage. Advances in polymer technology, 2020.

[9] Salunkhe, P.B. and Shembekar, P.S., 2012. A review on effect of phase change material encapsulation on the thermal performance of a system. Renewable and sustainable energy reviews, 16(8), pp.5603-5616.

[10] Sarkar, J., Ghosh, P. and Adil, A., 2015. A review on hybrid nanofluids: recent research, development and applications. Renewable and Sustainable Energy Reviews, 43, pp.164-177.

[11] Goudarzi, S., Shekaramiz, M., Omidvar, A., Golab, E., Karimipour, A. and Karimipour, A., 2020. Nanoparticles migration due to thermophoresis and Brownian motion and its impact on Ag-MgO/Water hybrid nanofluid natural convection. Powder Technology, 375, pp.493-503.

[12] Gupta, M., Singh, V., Kumar, R. and Said, Z., 2017. A review on thermophysical properties of nanofluids and heat transfer applications. Renewable and Sustainable Energy Reviews, 74, pp.638-670.

[13] Angayarkanni, S.A. and Philip, J., 2015. Review on thermal properties of nanofluids: Recent developments. Advances in colloid and interface science, 225, pp.146-176.

[14] Albojamal, A. and Vafai, K., 2017. Analysis of single phase, discrete and mixture models, in predicting nanofluid transport. International Journal of Heat and Mass Transfer, 114, pp.225-237.

[15] J. Buongiorno, Convective transport in nanofluids, 2006.

[17] Buongiorno, J., Venerus, D.C., Prabhat, N., McKrell, T., Townsend, J., Christianson, R., Tolmachev, Y.V., Keblinski, P., Hu, L.W., Alvarado, J.L. and Bang, I.C., 2009. A benchmark study on the thermal conductivity of nanofluids. Journal of Applied Physics, 106(9).

[18] Garoosi, F., Garoosi, S. and Hooman, K., 2014. Numerical simulation of natural convection and mixed convection of the nanofluid in a square cavity using Buongiorno model. Powder technology, 268, pp.279-292.

[19] Vahedi, B., Golab, E., Sadr, A.N. and Vafai, K., 2022. Thermal, thermodynamic and exergoeconomic investigation of a parabolic trough collector utilizing nanofluids. Applied Thermal Engineering, 206, p.118117.

[20] R.O. Sayyar, M. Saghafian, Numerical simulation of convective heat transfer of nonhomogeneous nanofluid using Buongiorno model, Heat Mass Transf. 53 (8) (2017) 2627–2636.

[21] Jasak, H., Jemcov, A. and Tukovic, Z., 2007, September. OpenFOAM: A C++ library for complex physics simulations. In *International workshop on coupled methods in numerical dynamics* (Vol. 1000, pp. 1-20).

[22] Jasak, H., 2009. OpenFOAM: open source CFD in research and industry. *International Journal of Naval Architecture and Ocean Engineering*, *1*(2), pp.89-94.

[23] Cardiff, P., Karač, A., De Jaeger, P., Jasak, H., Nagy, J., Ivanković, A. and Tuković, Ž., 2018. An open-source finite volume toolbox for solid mechanics and fluid-solid interaction simulations. arXiv preprint arXiv:1808.10736.

[24] https://www.openfoam.com/industries/ventilation

[25] N. G. Jacobsen, D. R. Fuhrman, and J. Fredsøe. A wave generation toolbox for the opensource CFD library: OpenFOAM. International Journal for Numerical Methods in Fluids, 70(9):1073–1088, 2012. doi: 10.1002/fld.2726.

[26] H. Elsafti and H. Oumeraci. A numerical hydro-geotechnical model for marine gravity structures. Computers and Geotechnics, 79:105 – 129, 2016. doi: http://dx.doi.org/10.1016/ j.compgeo.2016.05.025.

[27]] P. Horgue, C. Soulaine, J. Franc, R. Guibert, and G. Debenest. An open-source toolbox for multiphase flow in porous media. Computer Physics Communications, 187:217 – 226, 2015. doi: http://dx.doi.org/10.1016/j.cpc.2014.10.005

[28] Golab, E., Goudarzi, S., Kazemi-Varnamkhasti, H., Amigh, H., Ghaemi, F., Baleanu, D. and Karimipour, A., 2021. Investigation of the effect of adding nano-encapsulated phase change material to water in natural convection inside a rectangular cavity. Journal of Energy Storage, 40, p.102699.

[29] R. Hamilton, O. Crosser, Thermal conductivity of heterogeneous two component systems, I and EC Fundamentals 125 (3) (1962) 187–191.

[30] J.C. Maxwell, A Treatise on Electricity and Magnetism, second ed., Oxford University Press, Cambridge, UK, 1904.

[31] Xuan, Y., Li, Q. and Hu W., Aggregation structure and thermal conductivity of nanofluids, Journal of American Institute of Chemical Engineers (AIChE), Vol. 49(4), pp. 1038-1043, 2003.

[32] S.P. Jang, S.U.S. Choi, Effects of various parameters on nanofluid thermal conductivity, J. Heat Transfer 129 (2007) 617–623.

[33] Kumar, D. H., Patel, H. E., Kumar, V. R. R., Sundararajan, T., Pradeep, T., and Das, S. K., Model for heat conduction in nanofluids, Physical Review Letters, vol. 93, no. 14, pp. 144301-1–144301-4, 2004.

[34] J. Koo, C. Kleinstreuer, A new thermal conductivity model for nanofluids, J. Nanoparticle Res. 6 (2004) 577–588.

[35] R. Prasher, P. Bhattacharya, P.E. Phelan, Brownian-motion-based convective– conductive model for the effective thermal conductivity of nanofluids, J. Heat Transfer 128 (2006) 588–595.

[36] C.H. Chon, K.D. Kihm, S.P. Lee, S.U.S. Choi, Empirical correlation finding the role of temperature and particle size for nanofluid (Al2O3) thermal conductivity enhancement, Appl. Phys. Lett. 87 (15) (2005) 153107

[37] Xu, J., Yu, B., Zou, M. and Xu, P., A new model for heat conduction of nanofluids based on fractal distributions of nanoparticles, Journal of Applied Physics, Vol. 39, pp. 4486-4490, 2006.

[38] Evans, W., Fish, J. and Keblinski, P., Role of Brownian motion hydrodynamics on nanofluids thermal conductivity, Applied Physics Letters, Vol. 88, pp. 93-116, 2006.

[39] Yang, B., Thermal conductivity equations based on Brownian motion in suspensions of nanoparticles (nanofluids), Journal of Heat Transfer, vol. 130, no. 4, pp. 042408-1–042408-5, 2008.

[40] Corcione, M., Empirical correlating equations for predicting the effective thermal conductivity and dynamic viscosity of nanofluids, Energy Conversion and Management, Vol. 52, pp. 789–793, 2011.

[41] C-W. Nan, G. Liu, Y. Lin, M. Li, Interface effect on thermal conductivity of carbon nanotube composites, Appl. Phys. Lett. 85 (2004) 3549-3551.

[42] Q.Z. Xue, Model for thermal conductivity of carbon nanotube-based composites, Phys. B: Condens. Matter, 368 (2005) 302-307.

[43] H.E. Patel, K.B. Anoop, T. Sundararajan, S.K. Das, Model for thermal conductivity of CNT-nanofluids, Bull. Mater. Sci., 31 (2008) 387-390.

[44] S.M.S. Murshed, K.C. Leong, C. Yang, Inverstigations of thermal conductivity and viscosity of nanofluids, Int. J. Thermal Sci., 47 (2008) 560-568.

[45] Walvekar, R., Faris, I.A. and Khalid, M., 2012. Thermal conductivity of carbon nanotube nanofluid experimental and theoretical study. Heat Transfer—Asian Research, 41(2), pp.145-163.

[46] Einstein, A.: Eineneuebestimmung der molekuॅldimensionen. Annals. Phys. 324(2), 289–306 (1906)

[47] Mooney, M.: The viscosity of a concentrated suspension of spherical particles. J. Colloid Sci. 6(2), 162–170 (1951)

[48] Krieger, I.M., Thomas, J.D.: A mechanism for non-Newtonian flow in suspensions of rigid spheres. Transactions Soc. Rheol. 3(1), 137–152 (1957)

[49] Nielsen, L.E.: Generalized equation for the elastic moduli of composite materials. J. Appl. Phys. 41(11), 4626–4627 (1970)

[50] Batchelor, G.K.: The effect of Brownian motion on the bulk stress in a suspension of spherical particles. J. Fluid Mech. 83(01), 97–117 (1977)

[51] Brinkman, H.C.: The viscosity of concentrated suspensions and solutions. J. Chem. Phys. 20(4), 571 (1952)

[52] Graham, A.L.: On the viscosity of suspensions of solid spheres. Appl. Sci. Res. 37(3-4), 275–286 (1981)

[53] Kitano, T., Kataoka, T., Shirota, T.: An empirical equation of the relative viscosity of polymer melts filled with various inorganic fillers. Rheologica. Acta. 20(2), 207–209 (1981)

[54] Chen, H., Ding, Y., Tan, C.: Rheological behaviour of nanofluids. New J. Phys. 9(10), 367 (2007)

[55] Masoumi, N., Sohrabi, N., Behzadmehr, A.: A new model for calculating the effective viscosity of nanofluids. J. Phys. D.Appl. Phys. 42(5), 055501 (2009)

[56] Corcione, M., 2011. Empirical correlating equations for predicting the effective thermal conductivity and dynamic viscosity of nanofluids. *Energy conversion and management*, *52*(1), pp.789-793.

[57] Devi, S.A.; Devi, S.S.U. Numerical investigation of hydromagnetic hybrid Cu–Al2O3/water nanofluid flow over a permeable stretching sheet with suction. Int. J. Nonlinear Sci. Numer. Simul. 2016, 17, 249–257.

[58] Chougule, S.S.; Sahu, S.K. Model of heat conduction in hybrid nanofluid. In Proceedings of the 2013 IEEE International Conference on Emerging Trends in Computing, Communication and Nanotechnology (ICECCN), Tirunelveli, India, 25–26 March 2013; IEEE: New York, NY, USA; pp. 337–341.

[59] Wohld, J., Beck, J., Inman, K., Palmer, M., Cummings, M., Fulmer, R. and Vafaei, S., 2022. Hybrid Nanofluid Thermal Conductivity and Optimization: Original Approach and Background. Nanomaterials, 12(16), p.2847.

[60] Asadi, A., Asadi, M., Rezaei, M., Siahmargoi, M. and Asadi, F., 2016. The effect of temperature and solid concentration on dynamic viscosity of MWCNT/MgO (20–80)–SAE50 hybrid nano-lubricant and proposing a new correlation: An experimental study. International Communications in Heat and Mass Transfer, 78, pp.48-53.

[61] Khashi'Ie, N.S., Arifin, N.M., Pop, I., Nazar, R., Hafidzuddin, E.H. and Wahi, N., 2020. Thermal Marangoni flow past a permeable stretching/shrinking sheet in a hybrid Cu-Al. Sains Malaysiana, 49(1), pp.211-222.

[62] Batchelor, G., 1976. Brownian diffusion of particles with hydrodynamic interaction. Journal of Fluid Mechanics, 74(1), pp.1-29.

[63] McNab, G.S. and Meisen, A., 1973. Thermophoresis in liquids. Journal of Colloid and Interface Science, 44(2), pp.339-346.

[64] Brock, J.R., 1962. On the theory of thermal forces acting on aerosol particles. Journal of Colloid Science, 17(8), pp.768-780.

[65] Talbot, L.R.K.R.W.D.R., Cheng, R.K., Schefer, R.W. and Willis, D.R., 1980. Thermophoresis of particles in a heated boundary layer. Journal of fluid mechanics, 101(4), pp.737-758.

[66] S.Y. Motlagh, H. Soltanipour, Natural convection of Al2O3-water nanofluid in an inclined cavity using Buongiorno's two-phase model, Int. J. Therm. Sci. 111 (2017) 310–320.

[67] Heris, S.Z., Etemad, S.G. and Esfahany, M.N., 2006. Experimental investigation of oxide nanofluids laminar flow convective heat transfer. *International communications in heat and mass transfer*, **33(4)**, pp.529-535.

[68] Kamkari, B., Shokouhmand, H. and Bruno, F., 2014. Experimental investigation of the effect of inclination angle on convection-driven melting of phase change material in a rectangular enclosure. *International Journal of Heat and Mass Transfer*, **72**, pp.186-200.

[69] Kahveci, K., 2010. Buoyancy driven heat transfer of nanofluids in a tilted enclosure. *Journal of Heat Transfer*, *132*(6).

[70] Motlagh, S.Y., Golab, E. and Sadr, A.N., 2019. Two-phase modeling of the free convection of nanofluid inside the inclined porous semi-annulus enclosure. International Journal of Mechanical Sciences, 164, p.105183.

[71] Goudarzi, S., Shekaramiz, M., Omidvar, A., Golab, E., Karimipour, A. and Karimipour, A., 2020. Nanoparticles migration due to thermophoresis and Brownian motion and its impact on Ag-MgO/Water hybrid nanofluid natural convection. Powder Technology, 375, pp.493-503.

[72] Rösler, F. and Brüggemann, D., 2011. Shell-and-tube type latent heat thermal energy storage: numerical analysis and comparison with experiments. Heat and mass transfer, 47, pp.1027-1033.

[73] Kuznetsov, A.V., 2010. The onset of nanofluid bioconvection in a suspension containing both nanoparticles and gyrotactic microorganisms. International Communications in Heat and Mass Transfer, 37(10), pp.1421-1425.

[74] Bees, M.A., 2020. Advances in bioconvection. Annual Review of Fluid Mechanics, 52, pp.449-476.

[75] Shi, Q.H., Hamid, A., Khan, M.I., Kumar, R.N., Gowda, R.P., Prasannakumara, B.C., Shah, N.A., Khan, S.U. and Chung, J.D., 2021. Numerical study of bio-convection flow of magneto-cross nanofluid containing gyrotactic microorganisms with activation energy. Scientific Reports, 11(1), p.16030.

[76] Jafarzadeh, S., Sadr, A.N., Kaffash, E., Goudarzi, S., Golab, E. and Karimipour, A., 2020. The effect of hematocrit and nanoparticles diameter on hemodynamic parameters and drug delivery in abdominal aortic aneurysm with consideration of blood pulsatile flow. Computer Methods and Programs in Biomedicine, 195, p.105545.

[77] Abbasi, M., Esfahani, A.N., Golab, E., Golestanian, O., Ashouri, N., Sajadi, S.M., Ghaemi, F., Baleanu, D. and Karimipour, A., 2021. Effects of Brownian motions and thermophoresis diffusions on the hematocrit and LDL concentration/diameter of pulsatile non-Newtonian blood in abdominal aortic aneurysm. Journal of Non-Newtonian Fluid Mechanics, 294, p.104576.

[78] Gopalakrishnan, S.S., 2014. Dynamics and stability of flow through abdominal aortic aneurysms (Doctoral dissertation, Université Claude Bernard-Lyon I).